Effect of graphene in laminated composites of natural materials

Marta Dias Silva
marta.dias.silva@tecnico.ulisboa.pt

Instituto Superior Técnico, Universidade de Lisboa, Portugal
November 2021

Abstract

Composite materials of sandwich structures have been increasingly sought in several areas due to their desirable properties, such as lightness, high strength, and durability. On the other hand, and with the innovation of technology, there has been the need to test the addition of new components to this type of materials, being graphene one of them. This work aimed to study the addition of graphene in the matrix of epoxy resin and subsequently understand what effects it can have in the final composite. One of the biggest challenges of working with graphene is the difficulty in obtaining a good dispersion between it and the matrix. Different dispersion methods were tested, and different graphene contents were studied. To understand the effect on dynamic and mechanical properties, DMA and bending tests were performed to the different matrix-graphene combinations. The results obtained were in line with the objectives set out and allowed us to conclude how graphene affects the matrix properties and to understand which is the best content to add to the final composite to obtain better properties.

Keywords: Graphene, epoxy resin, sandwich structure, graphene nanoplatelets (GNPs)

1. Introduction

In the world of materials science and engineering, the aim is always to achieve the best combination of properties of a material for a particular application. With this, composite materials (the union of two or more materials) have emerged, resulting in a material with improved properties. Since society is used to living off innovation and advances in technology, industries have been looking for lighter, tougher, thin, flexible, or rigid materials, in addition to resistant to heat and wear. Due to the scarcity of resources and the benefit of sustainability, you must choose strategies that use materials derived from renewable resources. As such, studies are already being carried out on the addition of graphene as a reinforcement of composite materials, which, due to its desirable attributes such as reduced weight, high mechanical strength, and durability, have become increasingly promising. Graphene is a very promising material that is already revolutionizing the industrial world.

However, for the reinforcement material to improve the properties of the composite, it is necessary to promote a good interaction between graphene and the matrix

and ensure that its dispersion is homogeneous and stable.

In this way the aim of this work was to study the incorporation of different amounts of graphene in the matrix of an epoxy resin and to optimise its curing process for subsequent application in a sandwich composite.

Sandwich panels consist of two or more materials with different properties, in an arrangement of overlapping layers, connected by an adhesive element.[1], [2]
The choice of cork as a core for sandwich composites is due to properties such as low density, high shear modulus, high shear strength, high stiffness, and good thermal and acoustic insulation characteristics.[3]
The preferential use of glass fibres in these composites is due to their high tensile strength, low cost, high chemical resistance and good acoustic, thermal and electrical insulating properties. [4], [5] As adhesive material it is common to use thermosetting polymers, being epoxy the most used.

Graphene is one of the carbon allotropes that has raised most interest in the last decade, not only from an academic point of view, but also considering its potential applications[6]. Graphene can be defined as a two-dimensional (2D) planar sheet, with a thickness of one atom, consisting of carbon atoms with sp2 bonds rearranged in a honeycomb-like structure in the shape of hexagons, giving it unique mechanical, electrical and thermal properties.[7]

The processes to obtain graphene can be grouped into two categories: top-down and bottom-up. In this work, graphene was produced by the LPE method. This method consists first in the dispersion of graphite in an organic solvent (in this case they used water) so that the energy barrier is removed, that is, so that the Van der Waals forces are weakened and can facilitate the separation of graphene. The graphite is then exfoliated by ultrasound to obtain individual graphene sheets in suspension. This process results in high quality graphene nanoplates (GNPs) that can be produced in multiple layers (monolayers or multilayers) or forms (dispersions or powders). [8]–[10]

2. Methodology

To study the influence of graphene addition to the final composite, the work was divided into three parts: firstly, a characterisation of the isolated epoxy resin was performed, followed by a study of the addition of graphene in different amounts to the resin and, finally, the mechanical properties of the final composite were studied.

2.1. Production of test specimens

2.1.1. Epoxy Resin (EP) Specimens

The resin used was EPOLIT RS 7720, consisting of two parts: part A consists of a mixture based on epoxy prepolymer and part B, being the hardener, consists of amines. To produce these specimens, first the amount of A was weighed, then the amount of B, and then the two parts were mixed with the aid of a mechanical stirrer for about 1 minute at a speed of 3000 rpm. After obtaining a homogeneous mixture, degassing was carried out in a vacuum system for 3 minutes to eliminate any bubbles present in the mixture.

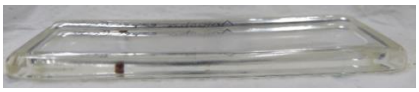

Figure 1 - Example EP resin specimen

2.1.2. Epoxy Resin (EP) with graphene nanoplatelets (GNPs) specimens

The GNPs used have a thickness of 10 nm and can present a size distribution between 3-15 µm. The production of these test specimens was identical to the previous one. For the graphene dispersion process four different methods were tested: manual dispersion, mechanical dispersion with VWR VOS 60 mechanical stirrer (3000 rpm for 1 min), dispersion with IKA Ultraturrax T18 homogeniser (3000 rpm for 10 min) and VWR ultrasonic dispersion (for 40 min).

Figure 2 - Example EP resin with GNPs specimen

2.1.3. *Sandwich* Composite

Two sandwich composites of conventional configuration were produced, composed of two faces of epoxy resin reinforced with fibreglass, separated by a core of cork agglomerate NL20 with 10 mm thick. The composite without graphene is designated as (C0) and the composite with graphene as (C1). Both configurations were produced by hand lay-up method.

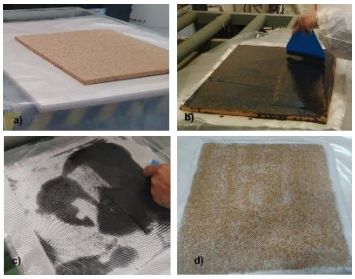

Figure 3 - Production of composites

2.2. Characterization methods

2.2.1. Fourier Transform Infrared Spectroscopy (FTIR)

All spectrums were obtained with the Perkin-Elmer Spectrum Two equipment with the Miracle ATR accessory from Pike, using 8 accumulation scans and 8 cm^{-1} of resolution. The chosen wavenumber range was 4000-400 cm^{-1}.

2.2.2. Dynamic Mechanical Analysis (DMA)

The tests were performed in the DMA equipment model Q800 from Thermal Analysis Instruments (TA analysis) that uses the TA AdvantageTM program to control the parameters. The type of clamps used was the dual cantilever and the tests were performed in multi-frequency mode (with controlled strain), and the temperature ramp mode was chosen. The tests were performed between 26-120°C, at a speed of 3°C/min and with amplitude and frequency of 15 µm and 1 Hz respectively. For this method, the resin and graphene specimens were cut to have the dimensions defined by ASTM D4065 (60 x 14 x 3 mm).

2.2.3. Scanning Electron Microscopy (SEM)

The equipment used was a FEG-SEM (Field Emission Gun Scanning Electron Microscope) JEOL JSM 7001F. The test specimens were broken in order to analyse the cross-sectional surface and were covered with a gold and palladium conductive coating. For a better analysis, the fractured specimens were placed vertically in the sample holder.

2.2.4. Three-Point Bending Test

This method is valid for thermosetting materials, and the bending stress is obtained according to ISO 178. The bending stress (σ_f) is calculated according to equation (1), where L is the distance between supports, F is the applied load, h is the thickness of the specimen and b is the width of the specimen.

$$\sigma_f = \frac{3FL}{2bh^2} \qquad (1)$$

The bending deformation (ε_f), on the other hand, can be calculated according to equations (2) where s corresponds to the deflection (mm).

$$\varepsilon_f = \frac{6sh}{L^2} \qquad (2)$$

The modulus of elasticity to bending is obtained by equation (3), where σ_{f1} is the measured stress for ε_1=0.0005 and σ_{f2} is the measured stress for ε_2=0.0025.

$$E_f = \frac{\sigma_2 - \sigma_1}{\varepsilon_2 - \varepsilon_1} \qquad (3)$$

These tests were performed in the Instron 5566 equipment, with a 500 N load cell. The specimens dimensions were defined according to ISO 178 (l = 80,0 ± 2,0 mm; b = 10,0 ± 0,2 mm; h = 4,0 ± 0,2 mm). For each of the specimens studied, average thickness measurements (h) were taken to subsequently adjust the loading span length and a velocity of 2 mm/min was set as referred to in ISO 178.[11]

2.2.5. Four-Point Bending Test

The calculation of the bending and shear stiffness of beams was based on previous studies.[12] Each specimen is tested with the same loading configuration (L) but incrementing the length of the support span (S=100 mm, S=150 mm, S=200 mm and S=250 mm). The test is performed at 40% of the maximum load, stopping before any deformation or permanent damage occurs in the faces or core of the sandwich structure.

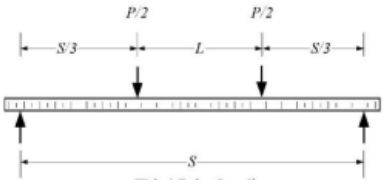

Figure 4 - Loading configuration[13]

Deducing the mid-span equation and replacing L=S/3, considering the configuration of Figure 4, it is possible to obtain the deflection at mid-span (Δ) as a function of the applied load (P), the bending stiffness (D) and the shear stiffness (U), which can be transformed into an equation of the type y=mx+q (equation 4).

$$\frac{\Delta}{P} = \frac{1.7}{96D}S^2 + \frac{1}{6U} \qquad (4)$$

Plotting the graph of equation (4) as a function of the span length (S2), a linear regression can be plotted to calculate D and U respectively through equations (5 and 6), where m and q are respectively the slope and intercept of the linear regression.

$$D = \frac{1.7}{96m} \qquad (5)$$

$$U = \frac{1}{6q} \qquad (6)$$

2.2.6. Shore D Hardness

Shore hardness tests were carried out using a Shore D durometer and for each test values were measured at three different points.

3. Results and discussion

3.1. Epoxy Resin

3.1.1 Cure (C) and Post-Cure (PC) Study

The curing process of the epoxy resin with the amines can be described in two steps: first, an epoxy group reacts with a primary amine, producing a secondary amine, which in a second step reacts with another epoxy group forming a tertiary amine. Therefore, it is possible to monitor the curing process, as the reactions involved result in a decrease in the epoxy and amine functional groups, reflected in a decrease in the intensities of their characteristic bands.

For evaluating the best curing time of the epoxy resin, we monitored the evolution of the visible band at 915 cm^{-1} corresponding to the deformation of the C-O bond of the epoxy ring. According to figure 5 the intensity of this band decreases with increasing curing time, and for longer times it is practically no longer visible.

As the curing reaction proceeded, new bonds were formed and reflected in the spectrum with the appearance of absorptions in the 3500-3400 cm-1 range (Figure 6). The bands appearing in this absorption range are difficult to quantify/analyse as they may correspond to O-H bonds resulting from ring opening to the presence of moisture in the sample, or to N-H bonds from secondary amines that may have been formed during the curing reaction.

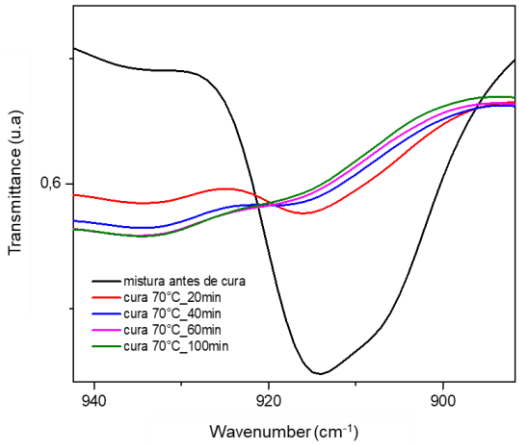

Figure 5 - Evolution of the absorption band of the C-O bond of the epoxy ring

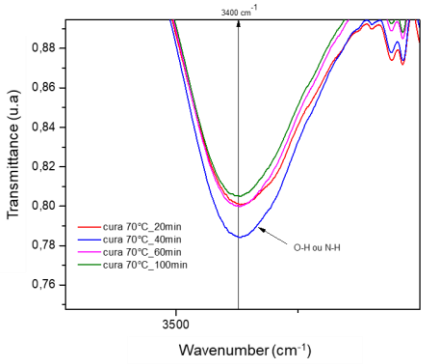

Figure 6 - Evolution of the absorption band of the O-H or N-H bonds

With this method it was concluded that after 60 min of curing there were no more epoxy rings left unreacted due to the intensity of the characteristic band of these rings being practically null.

Another method used was DMA, whose objective was to determine the highest value of glass transition temperature (Tg). The tan delta curves obtained show that the polymers were not completely cured, given the existence of two peaks. These peaks suggest that the material presents zones with different degrees of crosslinking, i.e. there are zones in which the chains can still move (first peak - lower Tg) and other

zones with maximum crosslinking (second peak - higher Tg).

In this way, it was necessary to apply a post-curing treatment that allowed tan delta curves to be obtained with only one well-defined peak and associated with a higher Tg, showing that the EP polymers were fully cured

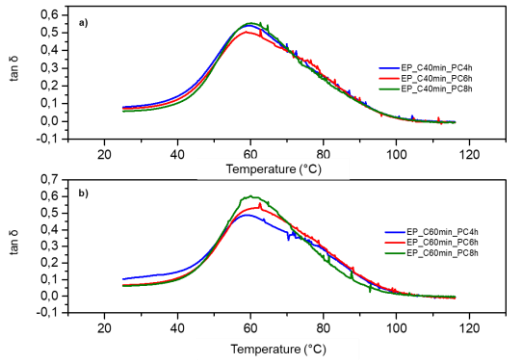

Figure 7 - Tan δ curves of EP with post-cure 4,6,8 h at 60 °C: a) cure 40 min e b) cure 60 min

So, the curing cycle chosen for the EP resin was 60 minutes at 70 °C followed by a post-cure of 6h at 60 °C.

3.2. Epoxy Resin with Graphene

3.2.1 Study of the methods of dispersion of graphene

For this analysis, the SEM technique was used, and the content chosen to compare the different methods was 3% GNPs. However, the analysis was inconclusive, as there are no significant differences between methods. As such and given that in terms of procedures is always preferable a faster and less expensive method, manual dispersion was chosen for the remaining tests, since it is the one that takes less time and has no associated energy costs.

3.2.2 Choosing the best graphene content

To choose the best GNP content to add to the epoxy matrix (EP) and subsequently to the final composite under study, it was necessary to study what influence it could have on the curing cycle of the resin (thermal properties) and on its mechanical properties.

The spectra obtained by FTIR for the different contents of GNPs using the defined curing cycle for the isolated EP resin, showed that there were no changes in relation to those of the pure EP. This means that there were no chemical bonds between the matrix and the graphene. It can also be seen that for any of the contents the peak corresponding to the C-O bond of the epoxy ring (at 915 cm-1) is not present, showing that the curing reaction occurred in totality.

For a better understanding of the type of interaction between the graphene and the EP matrix and how it may interfere in the dynamic-mechanical behaviour a new DMA analysis was performed. The curing cycle chosen was the pure EP resin (C60min_70°C + PC6h_60°C). The values in table x, show that regardless of the GNPs content, all presented E' values higher than those presented by the pure EP. This increase in E' value is related to the increase of stiffness of the polymeric matrix, which shows a good interaction between the GNPs and the matrix. The low value of E' for the composite with 1%GNPs, may be related to some problem associated with its production, as for example, a bad dispersion or some failure in degassing that may have originated the formation of bubbles and

consequently caused a bad interaction between matrix and GNPs.

Table 1- Resume of DMA parameters

Speciment	E' (MPa)	T_g 1st peak Tan δ (°C)	T_g 2nd peak Tan δ (°C)
EP	700	62,8	-
EP0.5%G	1042	59-60	80,5
EP1%G	880		
EP3%G	1158		

For all the composites with GNPs, a second peak appeared (elevation more below the main peak) at a higher Tg in the Tan δ curves. This phenomenon is because the presence of GNPs, act as anchorage points, due to the adhesion between the reinforcement and the matrix, restricting the movement of the polymer chains segments and contributing to a higher stiffness of the material. On the other hand, it is suggested that there are regions where the interface between GNPs and matrix was weak promoting molecular rearrangements. Such behaviour justifies the first peak at lower Tg.

This DMA analysis did not allow clarifying which graphene content to choose for the final composite but allowed concluding that the presence of graphene resulted in an overall strengthening effect and increase of Tg.

For the same curing cycle, the hardness was also measured. The results obtained showed that the composite with 1% of GNPs was the one that presented the highest hardness. In terms of average values, it was reflected in an increase of 31% when compared to the value of the pure EP.

Table 2 - Shore D hardness values obtained for polymers (C60min + PC6h)

	Hardness (Shore D)
EP	52,0 ± 4,6
EP0.5%G	61,0 ± 5,5
EP1%G	68,0 ± 4,4
EP3%G	58,0 ± 4,8

To understand the behaviour of the polymers reinforced with GNPs, the three-point bending tests were performed for two CP times. As can be seen in Figure 8, for both 6h and 10h, the flexural strength for the polymers reinforced with 0.5% and 3% GNPs tended to decrease, while for the polymer reinforced with 1% GNPs it tended to increase compared to the pure EP polymer. In the case of the polymer with 0.5%GNPs the lower value than the pure EP may be due to several factors. The fact of being such a low amount may have resulted in a weak interaction between matrix and GNPs, possibly enhanced by a non-uniform dispersion of GNPs. The polymer with more reinforcement (3% GNPs) resulted in the lowest value of flexural strength, and this phenomenon may be associated with the presence of agglomerates that become obstacles to the mobility of the chains, giving rise to the formation of voids between the matrix and GNPs.

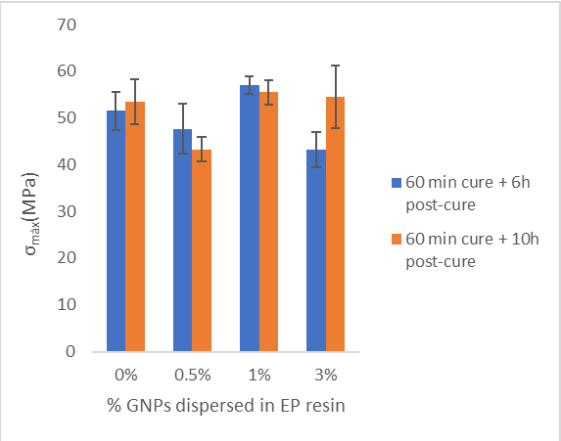

Figure 8 - Maximum bending stress for polymers studied for PC times of 6h and 10h

Another important parameter to evaluate is the flexural modulus of elasticity (Ef), figure 9. For 10h it presents a tendency to increase with the progressive increase of the GNPs content. This phenomenon is a result of the hardening effect caused by the high storage modulus (E') of the samples with 3% GNPs. For 6h, the highest value of Ef was obtained for the 1% GNPs reinforcement. This phenomenon may be associated with the fact that optimal material conditions, dispersion method and curing and post-curing conditions were used. Thus, the bending tests showed better results for the reinforcement with 1% GNPs and for a post-curing of 6h.

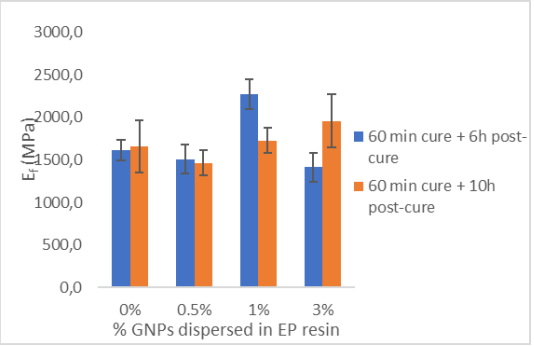

Figure 9 - Flexural Modulus of elasticity for polymers studied for PC times of 6h and 10h

Figure 10(a) corresponds to the pure PE polymer and reveals a smooth and mirror-like fractured surface showing that cracks spread freely and randomly. Whereas Figure 10(b) shows the laminar microstructure of the GNPs.

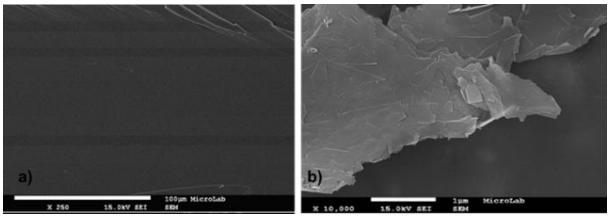

Figure 10 - SEM images of the fractured surfaces of pure EP (a) and GNPs (b)

Unlike the pure EP surface, the surfaces of the composites are rough due to the presence of GNPs. As it is known, the EP resins are fragile, but with the regions rich in GNPs promote the deviation of cracks generating irregular lines throughout the surface (white areas visible in the photomicrographs). Figure 4.19 (e-f) shows the emergence of regions with agglomerates making the surface rougher. This implies that the presence of reinforcement generates discontinuities and alters the fracture mode of the material.

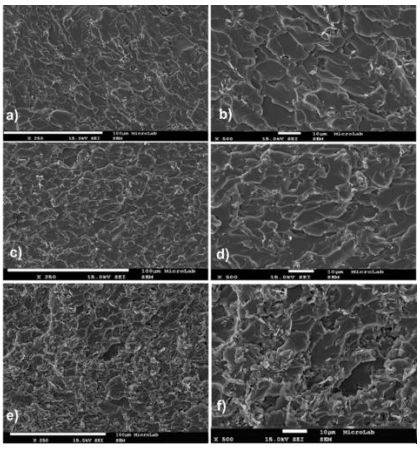

Figure 11 - SEM images of the fractured surfaces of GNPs/EP composites for magnifications x250

(left) and x500 (right): 0.5% m/m (a,b); 1% m/m (c,d) and 3% m/m (e,f);

After the analysis of the results of the mechanical tests and the analysis of the SEM images, we proceeded to the production of the final laminated composite choosing the 1% content to disperse in the matrix and the curing cycle of 60 min at 70 °C and 6h at 60°C.

3.3. Laminated Composite

3.3.1. Study of mechanical properties

According to the procedure described in 2.2.4, the maximum load value was determined for two specimens of each configuration for the support span S=250 mm. However, since several specimens were studied, the configurations should not be compared based on the maximum load supported, but rather convert these units into stiffness. This conversion to stiffness resulted in the results that are visible in table 3.

Table 3 - Bending stifness

	C0	**C1**
Bending stifness (MPa)	38 ± 10	43 ± 20

After these tests, the failure mode identified for both configurations were the same, corresponding to a failure of the faces under one of the rollers.

3.3.2. Production Cost

Cost is an important aspect in the choice of material. For this analysis it is necessary to know the cost of the constituent materials used in the design of the composite. After that, considering the amount of materials required for each configuration, it is possible to estimate the cost per m^2 of the configurations (table 4).

Table 4 - Configurations Cost

	C0	**C1**
Cost (€/m²)	41,50	45,82

4. Conclusions

The main objective of this work was to understand the influence of the graphene addition on the polymeric matrix faces in the final properties of the composite. The graphene contents studied were three (0.5, 1 and 3 % m/m), being that it was first studied the influence in the epoxy matrix, and only then, and for a chosen content, proceeded to the tests in the composite.

By FTIR analysis, the disappearance of the band corresponding to the C-O bond of the oxirane group (915 cm-1) allowed concluding that the EP resin had already undergone the full curing process at 60 min. On the other hand, through DMA analysis it was observed that it was necessary to submit the resin to a post-curing process, concluding that to obtain the highest Tg value (62.8 °) 6h were necessary, thus defining the EP resin curing cycle (60 min curing at 70 °C + 6h post-curing at 60 °C).

To study the mechanical properties of polymers with and without reinforcement, 3-point bending tests were performed. This analysis allowed the conclusion that for very low or very high GNPs contents, the interaction between the matrix and the

reinforcement is not the most adequate and may lead to undesired results. So, the 1% content of GNPs was the most appropriate.

Regarding the composite configurations studied, it is concluded that the configuration with graphene (C1) presented a higher stiffness compared to the conventional configuration (C0). Thus, the formulations tested resulted in a 12% increase in stiffness value and consequently an increase of more than 10% in cost.

References

[1] J. Arbaoui, H. Moustabchir, C. I. Pruncu, and Y. Schmitt, "Modeling and experimental analysis of polypropylene honeycomb multi-layer sandwich composites under four-point bending," *J. Sandw. Struct. Mater.*, vol. 20, no. 4, 2018, doi: 10.1177/1099636216659779.

[2] H. G. Allen, *Analysis and Design of Structural Sandwich Panels*. 1969.

[3] A. B. Strong, *Fundamentals of Composites Manufacturing, Materials, Methods and Applications*, vol. 2, no. 2. 2007.

[4] M. S. Aslanova, "Glass Fibers.," *Strong Fibres*, vol. 21, no. Ref 19, pp. 3–60, 1985.

[5] P. K. Mallick, *Fiber-reinforced composites: Materials, manufacturing, and design, third edition*, 3th ed. 2007.

[6] 1 A. A. Firsov2 K. S. Novoselov, 1 A. K. Geim, 1* S. V. Morozov, 2 D. Jiang, 1 Y. Zhang, 1 S. V. Dubonos, 2 I. V. Grigorieva, "Electric field effect atomically thin carbon films," vol. 306, no. 2, pp. 666–669, 2017, doi: 10.1126/science.1102896.

[7] E. P. F. Cunha, "Funcionalização Química de Nanotubos de Carbono e Formação de Grafeno," Universidade do Minho, 2011.

[8] R. Bhoria, "Enhancing Liquid Phase Exfoliation of Graphene in Organic Solvents with Additives," *Enhancing Liq. Phase Exfoliation Graphene Org. Solvents with Addit.*, pp. 1–15, 2019, doi: 10.5772/intechopen.81462.

[9] N. Kumar *et al.*, "Top-down synthesis of graphene: A comprehensive review," *FlatChem*, vol. 27, pp. 2452–2627, 2021, doi: 10.1016/j.flatc.2021.100224.

[10] "No Title." www.graphenesq.com- (accessed Jun. 19, 2021).

[11] "BS EN ISO Plastics- Determination of flexural properties," ISO 178:2003,European Standard,2003.

[12] M. I. T. Ramos, "Produção e Caracterização de Materiais Compósitos à base de Aglomerado de Cortiça", Tese de Mestrado, IST, UL, Lisboa, Portugal, 2018..

[13] "Standard Test Method for Core Shear Properties of Sandwich Constructions by Beam", *Astm C393-06*, American Society for Testing and Materials, 2006